Bubble-bubble interactions and wall pressures/temperatures produced by the collapse of a bubble pair near a rigid surface

Shahaboddin A. Beig*; Eric Johnsen;

Mechanical Engineering Department, University of Michigan, Ann Arbor, MI, USA;

Abstract

Cavitation occurs in a variety of applications ranging from naval structures to biomedical ultrasound. One important consequence of cavitation is structural damage to neighboring surfaces following repeated inertial collapse of vapor bubbles. Although the mechanical loading produced by the collapse of a single bubble has been widely investigated, less is known about how the presence of a second bubble affects the loading. In such a problem, the bubble-bubble interactions modify the dynamics, e.g., by increasing the non-sphericity of the bubbles and amplifying/hindering the collapse intensity depending on the flow parameters. Here, we quantify the effects of bubble-bubble interactions on the bubble dynamics, as well as the pressures produced by the collapse of a pair of vapor bubbles near a rigid surface. We perform high-resolution simulations of this problem by solving the three-dimensional compressible Navier-Stokes equations for gas/liquid flows. The results are used to investigate the non-spherical bubble dynamics and characterize the pressure fields based on the relevant parameters entering the problem: stand-off distance from the wall surface, the angle, and the distance between the two bubbles.

Keywords: cavitation; bubble collapse; re-entrant jet; double jetting;

Introduction

In most applications, cavitation-induced damage is caused by the collapse of bubble clouds containing a large number of bubbles. Experimental observations reveal that the collapse of these clouds may emit intense pressures, and induce substantial structural damage [1,2]. Hansson *et al.* (1982) investigated the collapse of a hemispherical bubble cloud close to a rigid wall and illustrated that the collapse takes place in an inward fashion [3]. The subsequent inward-propagating shock wave concentrates the collapse energy in the cloud center, leading to the generation of high pressure regions. When a dense bubble cloud collapses near a rigid boundary, the combination of the interactions between the bubble cloud and the neighboring wall, and the interactions among the collapsing bubbles gives rise to bubble asymmetry, and the formation of re-entrant jets [4,5]. In such flows, bubble-bubble interactions may affect the overall dynamics, and must be accounted for to predict impact load, and subsequent cavitation erosion.

Owing to the complexity of these nonlinear flows, theoretical approaches are challenging. On the other hand, diagnosing these flows experimentally is not trivial, because of the wide range of spatial and temporal scales, difficult optical access, and lack of accuracy in measuring devices. Numerically resolving the full bubble cloud dynamics is not feasible at the present time. Therefore, these obstacles have triggered the development of simplified homogeneous-mixture models that are typically based on spherical bubble dynamics [6,7].These models neglect the non-spherical effects of the collapse and tend to overestimate the produced pressures at the collapse; in a numerical study, Tiwari *et al.* (2015) simulated the collapse of a hemispherical cluster containing 50 bubbles, and measured peak pressures for a variety of configurations over an order of magnitude lower than the values predicted by reduced cloud models [5].

To characterize bubble-bubble interactions and quantify their effects on the non-sphericity of the collapse and the resulting pressures, we carry out highly-resolved three-dimensional simulations of bubble pairs collapsing near rigid surfaces. We perform a parametric study and quantify the bubble morphologies and collapse non-sphericity, examine the radially propagating shocks, and report the pressures measured along the wall surface. By investigating interactions among the bubbles and the boundary and their effects on bubble dynamics, this study will provide

*Corresponding Author, Shahaboddin A. Beig: alahyari@umich.edu

knowledge necessary to develop reduced cloud models that takes the non-spherical effects of the collapse into account, and can be used to perform more realistic simulations.

Numerical method

A solution-adaptive central/discontinuity-capturing approach is employed to solve the compressible Navier-Stokes equations for a binary gas-liquid system [8]. In this problem, two bubbles with identical initial volume collapse in the vicinity of a rigid surface. The problem setup is shown in Figure 1. The bubble, located at distance H_o from the wall, is called the "primary bubble". The non-dimensional parameter $\delta_o = H_o/R_o$ defines the initial proximity of the primary bubble to the wall. The "secondary bubble"' is located at distance D_o from the primary bubble, such that the non-dimensional parameter $\gamma_o = D_o/R_o$ sets the distance between the two bubbles, and the connecting line makes the angle ϕ with the horizontal. Thus, δ_o, γ_o, and ϕ are the geometrical variables, determining the bubbles' configuration at the beginning of the collapse, and the driving pressure is set to $p_\infty = 5$ MPa. The problem has a plane of symmetry (the middle plane), so we simulate only half of the domain, with symmetric boundary condition along the corresponding plane. Non-reflecting boundary conditions are applied along the remaining boundaries, except for the no-slip, adiabatic wall. To study the effects of geometry on the bubble dynamics, the following parameter ranges are considered: $1.1 \leq \delta_o \leq 3.0$, $1.1 \leq \gamma_o \leq 3.0$, and $0° \leq \phi \leq 90°$. The total number of computational cells varies between 1 to 2 billion, depending on the geometrical configuration of the bubbles, such that there are 192 cells per initial bubble radius for all cases. The theoretical Rayleigh collapse time $t_c = 0.915R_o\sqrt{\rho_l/\Delta p}$, which is $t_c = 1.3\mu s$ for this problem, is used to non-dimensionalize time.
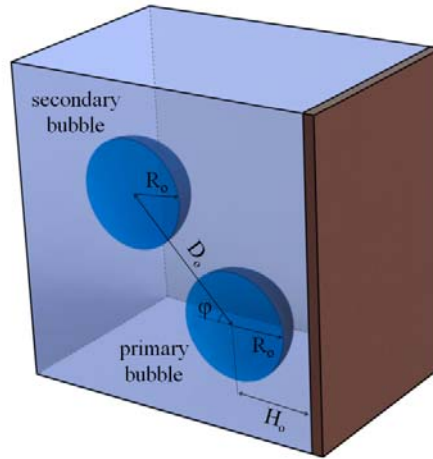

Figure 1. Schematic of the problem setup

Results: Qualitative dynamics

Figure 2 shows contours of density gradient magnitude, and pressure at different times during the collapse, where $\delta_o = 1.5$, $\gamma_o = 2.5$, and $\phi = 45°$. As the collapse starts, the bubbles release radially propagating rarefaction waves, which later interact with each other and the rigid wall. When the rarefaction impinges upon the bubble interface, a rarefaction is transmitted into the bubble, while a compression wave is reflected back due to the impedance mismatch. These continual interactions result in a zigzag wave pattern in the domain, which further accelerates the bubbles' interface non-uniformly ($t = 0.11$). The formation of a re-entrant jet towards the wall when a single bubble collapses near a rigid wall is thoroughly discussed in literature. A re-entrant jet is also observed in the collapse of bubble pairs in a free field, if occurring in-phase, and with bubbles relatively similar in size; in such a case, the jets accelerate towards each other. In this problem, unlike single bubble collapse near a rigid wall or the collapse of bubble pairs in a free field, the jet is directed neither towards the wall nor the other bubble, but in-between. Here, the jet forms within the secondary bubble first ($t = 1.12$). Upon the impact of the re-entrant jet onto the distal side of the secondary bubble, a water-hammer shock is generated, which, combined with the shock wave from the bubble implosion, creates a high-pressure region. The bubble then takes the form of a vortex ring migrating in the direction

of the jet angle. The re-entrant jet is observed to form within the primary bubble, tilted slightly away from the wall and towards the secondary bubble. Ultimately, the jet hits the distal side of the primary bubble, and creates a water-hammer shock. At this time, the shock from the collapse of the secondary bubble has reached the primary bubble and compresses it even more, resulting in a stronger collapse of the primary bubble, and thus producing high pressure regions ($t = 1.25$). Upon the impact of the shock emitted from the collapse of the secondary bubble, followed by the shock from the primary bubble collapse, high pressures are measured along the wall. The shock waves reflect back and eventually interact with the vortex rings again ($t = 1.41$). Although the major events during the collapse (e.g., jet formation, shock propagation, and vortex ring migration) are similar in single-bubble and twin-bubble problems, adding an extra bubble to the flow creates a far more complicated dynamics.
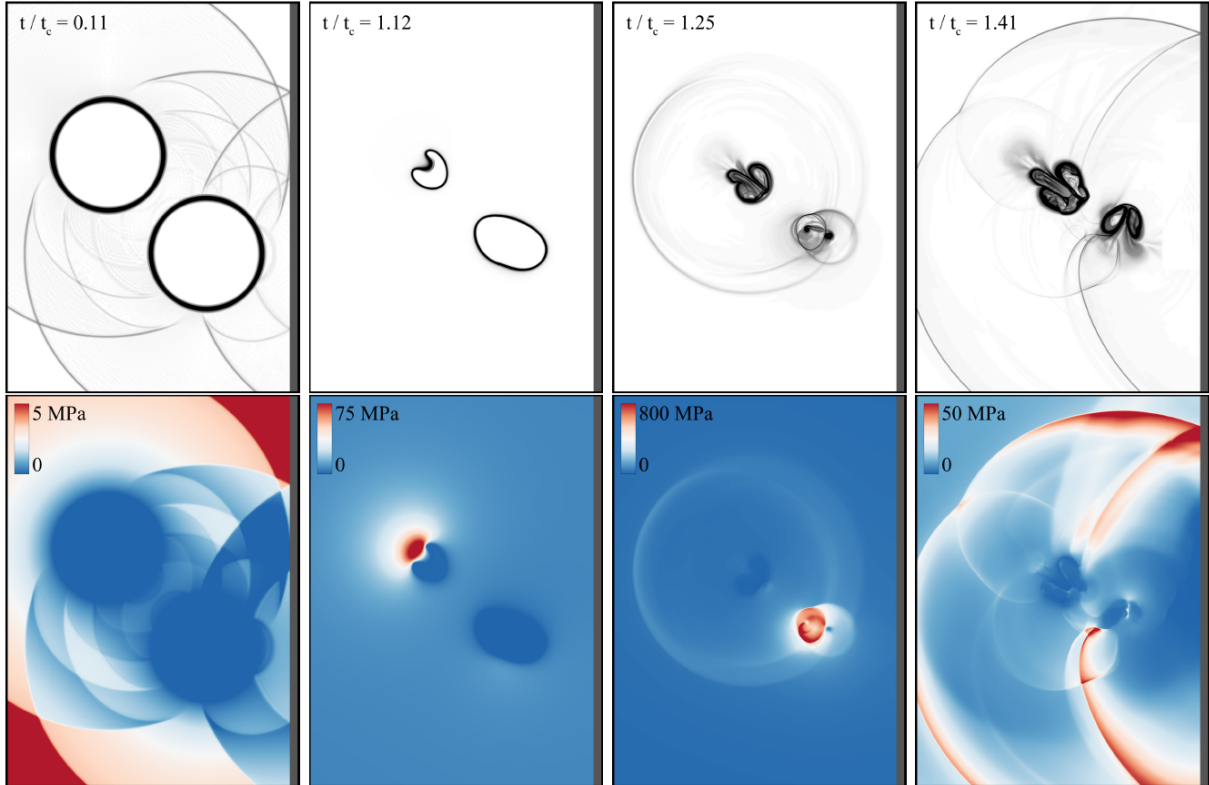

Figure 2. Collapse of a bubble pair near a rigid surface with $\delta_o = 1.5$, $\gamma_o = 2.5$, $\phi = 45°$, and $p_\infty = 5$ MPa; top: density gradient magnitude; bottom: pressure contours.

Results: Quantitative dynamics

The collapse of a bubble pair near a rigid surface combines two problems in which re-entrant jets form: collapse of a bubble next to another bubble and collapse of a bubble near a wall. Our numerical simulations show that the jets are formed within both primary and secondary bubbles, though with distorted shapes and geometry-dependent angles. One objective is to estimate the jet angle and the subsequent bubble migration angle based on the initial geometry of the system. Beig (2018) proposed the following theoretical model to estimate jet angles for both primary (α_1), and secondary (α_2) bubbles [9]:

$$\alpha_1 = \frac{\delta_o + 0.5\gamma_o}{\delta_o}(180° - \phi), \tag{1a}$$

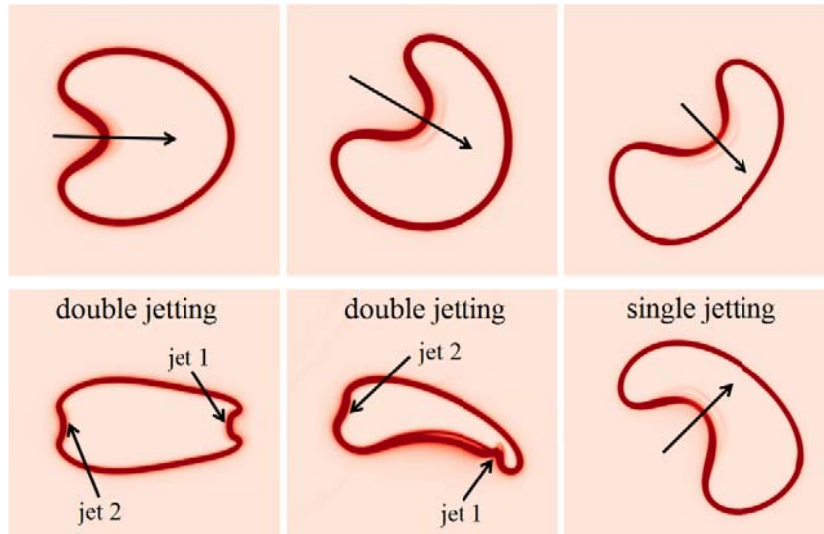$$\alpha_2 = \frac{\delta_o + \gamma_o(0.5 + cos\phi)}{\delta_o + \gamma_o cos\phi}\phi. \tag{1b}$$

Figure 3. jet morphology at different angles $\phi = 0°, 45°, 90°$ for secondary (top) and primary (bottom) bubbles with $\delta_o = 1.5$, and $\gamma_o = 2.5$.

According to the simulations, the secondary bubble collapses prior to the primary bubble for all configurations, except for $\phi = 90°$, in which case the two bubbles collapse at the same time. Although the two mechanisms inducing jet formation promote different angles, they are both on the right side of the secondary bubble. Thus, it is anticipated that, the jet points towards the bottom-right and that the vortex ring convects in that same direction. Figure 3 (top) shows the jet morphology immediately before impact at the top. The jet points in the direction perpendicular to the wall ($\alpha_2 = 0°$) at $\phi = 0°$, where the secondary bubble is located directly behind the primary bubble. By increasing the angle ϕ, the jet of the secondary bubble starts to turn away from the horizontal, and reaches the maximum absolute value of $\alpha_2 = 49°$, at $\phi = 90°$. This is shown further in Figure 4 (left), where we plot the jet angle (α_2), as a function of the initial configuration angle, ϕ. The results show a good agreement with the theoretical model. As expected, the absolute value of the jet angle increases by increasing the angle ϕ.

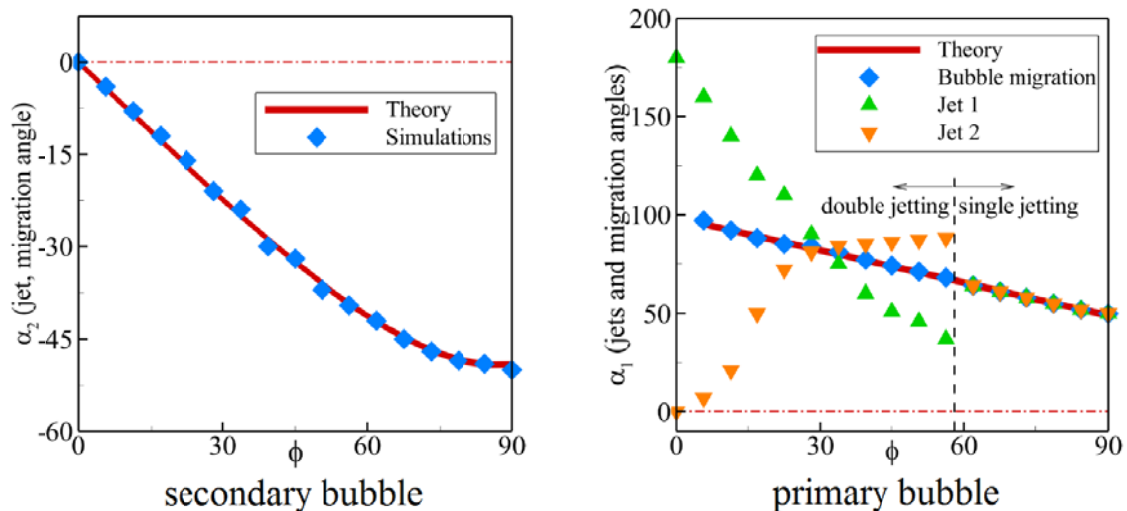

Figure 4. Jet and migration angles as a function initial angle ϕ for secondary (left) and primary (right) bubbles with $\delta_o = 1.5$, and $\gamma_o = 2.5$; red dashed-dotted line represents the jet angle in single bubble collapse.

Unlike the secondary bubble, the mechanisms leading to jet formation (presence of another bubble and of a wall) lie on opposite sides of the primary bubble, which can lead to a more non-spherical behavior and eventually complicate the dynamics further. Figure 3 (bottom) qualitatively illustrates the primary bubble shape, and the jet(s) formation, just before the impact. Figure 4 (right) also shows jet and migration angles versus the initial configuration angle, ϕ. According to the simulations, two re-entrant jets are observed to form within the primary bubble at $\phi = 0°$; one with angle $0°$, and the other one with angle $180°$ in the exact opposite direction. At $\phi = 45°$, "jet 1" is about to hit the distal side, while "jet 2" is still developing. However, for $\phi = 90°$, only one single jet at angle $\phi = 49°$ is observed. By increasing ϕ from $0°$ to $90°$, the jets start deforming, and ultimately at $\phi = 56°$, double-jetting no longer occurs and a single jet is observed. Although the theoretical model can predict the direction of the primary bubble migration after the collapse, it cannot determine the jet angles in the regime where double jetting occurs; after this threshold, a single jet is formed and the proposed model accurately describes the jet angle and, subsequently, the direction of the bubble migration. The emergence of double jetting affects the dynamics, the generated shock waves, and pressure loadings produced at the collapse; thus, the role of initial configuration (e.g., the arrangement of the bubbles and their proximity to the rigid wall) on the collapse non-sphericity and overall dynamics is non-negligible.

Results: Wall pressure

The wall pressure p_{mw} is a quantity of interest for erosion [10,11]. Figure 5 shows how this quantity depends on the angle. The maximum wall pressure behaves in a non-monotonic fashion: it initially increases and reaches a local maximum as the angle is increased; thereafter, it starts to decrease to a minimum value at $\phi = 75°$, and increases again thereafter to reach it highest value at $\phi = 90°$. For all cases, p_{mw} is lower than that of a single bubble, except for $\phi = 90°$ where the reported value is slightly higher than the pressure produced by a single bubble. In general, the presence of the secondary bubble lowers the impact loads along the wall surface.
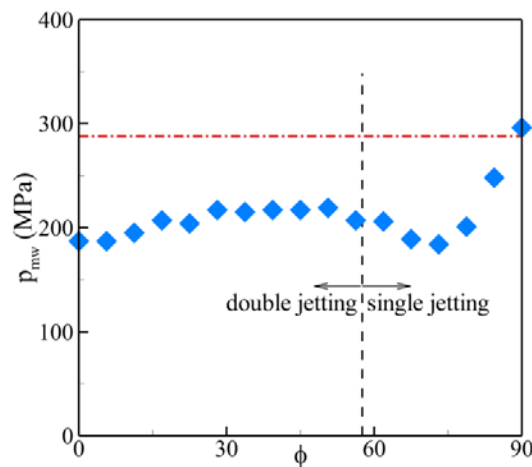

Figure 5. Maximum wall pressure as a function of the initial angle ϕ, with $\delta_o = 1.5$, $\gamma_o = 2.5$, and $p_\infty = 5$ MPa; red dashed-dotted line represents the collapse time in single bubble case.

Conclusions

In the collapse of bubble clouds, the inter-bubble interactions result in a complex non-spherical behavior and affect the collapse properties further. To quantify the effects of these interactions on bubble dynamics, we simulated the collapse of a pair of vapor bubbles near a rigid wall. We showed that if a second bubble is placed in the vicinity of the original bubble, the collapse becomes far more complicated. In fact, strong bubble-bubble interactions dramatically increase the non-sphericity of the bubbles, compared to the single bubble collapse. These interactions may amplify or reduce the pressures produced at the collapse, depending on the initial configuration of the problem. We showed that the maximum pressure along the wall behaves non-monotonically in the presence of the secondary bubble with varying angle. Distorted re-entrant jets were observed to form within both bubbles, and it was shown that depending on the geometrical configuration, two jets were detected penetrating the primary bubble, an event we

call "double jetting". Unlike single bubble case, the dynamics depend on at least three additional parameters (inter-bubble distance, relative size and angle), in addition to the stand-off distance and driving pressure. The results show that the dependence on even one of these parameters is complicated; determining the dependence on all parameters will be challenging. From this observation, it follows that the value of such high-resolution simulations to understand or predict the collapse of many bubbles (clouds) is questionable because there are too many parameters. As a result, modeling the behavior of clouds of bubbles in the context of erosion may require alternative approaches.

Acknowledgments

References

[1] Kubota, A., and Kato, H., Yamaguchi, H., and Maeda, M. (1989). *Unsteady structure measurement of cloud cavitation on a foil section using conditional sampling technique*. J. Fluids Eng., 111, 204–210.
[2] Ceccio, S. L., and Brennen, C. E., (1991). *Observations of the dynamics and acoustics of travelling bubble cavitation*. J. Fluid Mech., 233, 633–660.
[3] Hansson, I., Kedrinskii, V., and Morch, K. A. (1982). *On the dynamics of cavity clusters.* J. Phys. D: Appl. Phys., 15, 1725–734.
[4] Bremond, N., and Arora, M., and Ohl, C. D., and Lohse, D. (2006). *Controlled multibubble surface cavitation.* Phys. Rev. Lett., 96, 224501.
[5] Tiwari, A., Pantano, C., and Freund, J. B. (2015). *Growth-and-collapse dynamics of small bubble clusters near a wall.* J. Fluid Mech., 775, 1–23.
[6] Van Wijngaarden, L. (1968). *On the equations of motion for mixtures of liquid and gas bubbles*. J. Fluid Mech., 33, 465–474.
[7] Fuster, D., and Colonius, T. (2011). *Modelling bubble clusters in compressible liquids*. J. Fluid Mech., 688, 352–389.
[8] Beig, S. A., and Johnsen, E. (2015). *Maintaining interface equilibrium conditions in compressible multiphase flows using interface capturing.* J. Comput. Phys., 302, 548–566.
[9] Beig, S. A. (2018). *A computational study of the inertial collapse of vapor bubbles near a rigid surface.* PhD thesis, University of Michigan.
[10] Philipp, A., and Lauterborn, W. (1998). *Cavitation erosion by single laser-produced bubbles.* J. Fluid Mech., 361, 75–116.
[11] Johnsen, E., and Colonius, T. (2009). *Numerical simulations of non-spherical bubble collapse.* J. Fluid Mech., 629, 231–264.